Renewable Energy 125 (2018) 1003–1014

Contents lists available at ScienceDirect

Renewable Energy

journal homepage: www.elsevier.com/locate/renene

A new low-cost installation scheme of PATs for pico-hydropower to recover energy in residential areas

A. Carravetta [a], O. Fecarotta [a, *], H.M. Ramos [b]

[a] Department of Civil, Structure and Environmental Engineering, Università di Napoli Federico II, via Claudio, 21, 80125 Napoli, Italy
[b] Departamento de Engenharia Civil, Arquitectura e Georrecursos, InstitutoSuperiorTécnico, Avenida RoviscoPais, 1, 1049-001 Lisboa, Portugal

ARTICLE INFO

Article history:
Received 30 July 2017
Received in revised form
10 January 2018
Accepted 28 February 2018
Available online 2 March 2018

Keywords:
PATs
Pumps as turbines
Hydropower
Water networks
Energy recovery
Energy efficiency in water systems

ABSTRACT

A limiting factor in the use of hydropower plants in water supply networks consists in the cost of the electromechanical production device and the equipment necessary for the plant regulation. Pumps as Turbines (PATs) are electromechanical devices that have already been used in many mini and micro hydropower plants. Due to their low cost and reliability, PATs are an optimal solution for pico-hydropower plants, whose regulation has been widely analysed in literature, for power installations of only a few kW. A new power plant for small residential areas is presented herein. The new low-cost plant is provided with two PATs, that can work as single, series or parallel (SSP) turbines, and three on/off valves, whose synchronous operations regulate the flows and the head loss. The proposed design method is based on the maximization of the effectiveness of the system. Experimental data on a PAT are used to simulate the plant in several hydraulic conditions, with the application of the turbomachinery affinity law. The simple plant operations and the resulting interactions with the network confirm the viability of the proposed scheme. An economic assessment shows the feasibility of the new plant in different hydraulic situations.

1. Introduction

In water distribution networks (WDNs) pressure reducing valves are generally used to dissipate the excess hydraulic energy and set optimal pressure values to increase the system reliability and drastically reduce leakage [1–3]. Different strategies are proposed for the location of valves in a WDN [4–6].

Along the water pipelines, the energy that is dissipated by valves or within pressure break tanks could be recovered by substituting dissipation nodes with energy production nodes [7,8]. Several authors suggest the replacement of pressure regulating valves with turbines, considering that a turbine transforms hydraulic energy into electricity [9–11]. In such micro hydro power plants (HPP), with power capacities ranging between a few kilowatts and one hundred kilowatts, the use of a PAT in the production node is recommended on account of the lower cost of the pumps when compared to classic turbines [12–15]. Since the performance curves of pumps operating in turbine mode are generally not provided by the manufacturers, the selection of the most appropriate machine is difficult. Thus, several authors have addressed their research towards the investigation and prediction of the behaviour of PATs: Derakshan et al. (2012) [16] developed a semi-empirical model, based on a number of experimental tests, to predict the behaviour of a PAT based on the pump performance curves. Pugliese et al. (2016) [17] described the behaviour of two PATs under experimental tests and Kerschberger et al. (2010) [18] and Rodrigues et al. (2003) [19] developed some CFD calculations to investigate the performance of pumps when working in turbine mode.

In water distribution systems, variable operating conditions arise as a result of the daily pattern of water demand [10] and a PAT control system is needed to deal with such variation. Several works describe the difficulties arising when a pressure reducing valve is replaced by a turbine in a water distribution system: Fontana et al. (2016) [20] described a real-time control method for a turbine within a lab-scale water network and Arriaga et al. (2010) [14] and De Marchis et al. (2016) [21] investigated the mutual interaction between the energy production device and the water network. A number of recent works have investigated the problem of the optimal location of a turbine within a water network, to maximize either the leakage reduction or the energy production [22–25].

Among others, Carravetta et al. [26,27] proposed a regulation

* Corresponding author.
E-mail address: oreste.fecarotta@unina.it (O. Fecarotta).

https://doi.org/10.1016/j.renene.2018.02.132
0960-1481/

scheme to deal with the variability of both head and discharge, as presented in Fig. 1. In hydraulic regulation (HR), a bypass and two dissipation valves allow the PAT to work constantly near its best efficiency point (BEP), but for most of its operating time only a fraction of the power to be dissipated can be converted. In electric regulation (ER) the rotational speed is changed by a variable frequency driver, and all the energy is converted by the PAT; however, the working conditions can be far from the machine BEP for long periods. A third regulation scheme includes both hydraulic and electric regulation (HER) (Fig. 2), allowing a maximization of the energy production and system reliability, but with high equipment costs. Simplified schemes could be conceived in the absence of valve A or valve B in the HR or HER modes, or by inserting the PAT without any regulation, without a complete hydraulic equivalence, with a classic pressure reducing valve.

In HR mode, for a net-head ΔH^d, higher than the head-drop deliverable by the machine ΔH^T (at the left of the PAT characteristic curve in Fig. 2-a), the series valve dissipates the excess pressure ΔH^V. Instead, when the discharge Q^d is large (at the right of the PAT characteristic curve in Fig. 2-a), the PAT produces a head-drop higher than the available net-head: in this case, the parallel valve is opened to bypass a part of the discharge Q^b and reduce the discharge flowing into the PAT from Q^d to Q^T. Conversely, in ER mode (Fig. 2-b), the operating speed (N) of the generator is changed between N_{min} and N_{max} to match the load conditions determined by the instant flow discharge and head drop values; specifically, the PAT characteristic curve is modified to match the available head. Finally, in HER mode (Fig. 2-c), valve stroking and the operating speed can be selected to obtain the derivable high drop with the highest performance.

The variable operating strategy (VOS) is the design model proposed for PAT sizing [28]. Starting from the characteristic and efficiency curves of a single prototype pump in turbine mode, and from the daily pattern of flow rate and pressure variation, VOS will find the diameter of the PAT optimizing the HPP design. VOS can maximize either the plant capability, i.e. the energy production of the plant, or the plant effectiveness [29], when also the electromechanical reliability and the hydraulic sustainability of the plant are considered.

Using a design based on the application of VOS, the economic viability of a valve substitution with a PAT has recently been demonstrated with reference to a single dissipation node [30] or in the dynamic control of a WDN by the replacement of several pressure reducing valves [31].

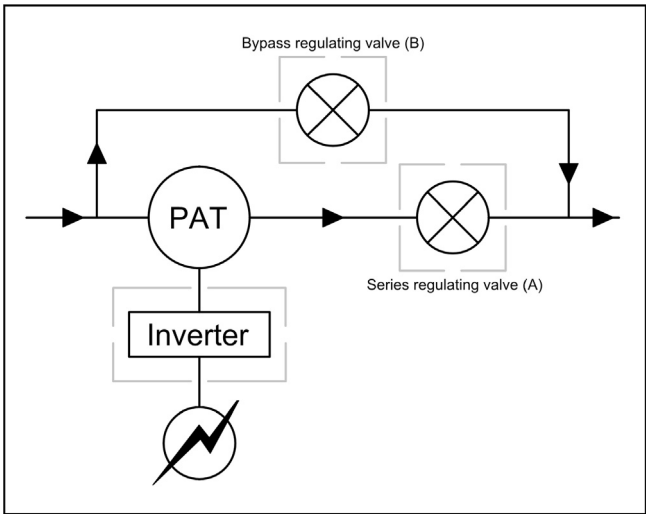

Fig. 1. Regulation control system to be applied in a PAT (from Ref. [26]).

Two factors exist limiting a wider diffusion of PATs: i) the cost of the regulations systems could be not convenient for a pico HPP, where the available power is small and variable [32]; and ii) the maintenance of regulation systems could be a concern for the technical management of a WDN [33].

A reduction of the plant cost is required also in the presence of intermittent energy production, as in the case of dynamic pressure control, where the pressure reducing valve could be totally closed during part of the day, or in irrigation [34] because the water distribution and, consequently the energy production, are limited to the summer months.

In this paper, a new design scheme for a HPP, which reduces the installation costs and simplifies the operations, is proposed for small residential area where a small tolerance in the service pressure is allowed. The simplified PAT regulation strategy, namely single-series-parallel (SSP) is a new regulation mode where the operation of three on/off valves, installed in a pipe circuit together with two PATs, allows a selection of the working mode, switching from a single turbine to two series turbines or to two parallel turbines. A sketch of the new plant is shown in Fig. 3 and the operation of the plant is presented in detail hereafter. The entire design of the plant is based on the maximization of the effectiveness of the system. The experimental data on a tested PAT are used to simulate different machines with the application of the turbomachinery affinity law. Several hydraulic patterns, with different values of maximum discharge and static head, are modelled, based on the frequency distribution of the discharge for small residential areas, according to the Monte Carlo model for extraction. The results of the optimized design are shown in terms of the energy produced, plant effectiveness and plant capability, for different load conditions. The resulting sequence of the three working conditions is simple and based only on the measured upstream pressure.

The economic feasibility, in terms of the net present value (NPV), is evaluated for the different load conditions and design solutions, and compared with the results of the VOS literature design method.

2. Discharge distribution in a small residential area

The design of a HPP should be based on direct measurements of the daily trends of flow rate and pressure in the dissipation node. In fact, the operational conditions are crucial in PAT design. For small urban areas, the daily flow pattern is very variable [35]. Fig. 4 [36,37] shows the different contributions of the various water customers to the total demand.

Based on the typical flow distribution of circulators in different building types (offices and hospitals), a standard frequency function of the part load, i.e. the fraction of the peak load Q_{load} (Fig. 5), has been proposed [38]. This distribution can be approximated by a lognormal probability density function ($m = -1{,}063$, $s = 0{,}516$). More recently [39], such a distribution has been used to model the water demand of a small residential area.

The supply pressure of small aggregates along the peripheral branches of a WDN is very variable, depending on several factors. High service pressures are preferred with well-managed networks and large water pressures at the network inlet. In the presence of high leakage, pressure control is recommended, and a much lower pressure value is available at the inlet of the residential area.

In small residential areas, the peak demand coefficient, defined as the ratio between the maximum and average flow rate can be very large, decreasing according to a power law with the number of inhabitants [40]. According to Fig. 4, the peak coefficient of hospitals and offices is close to 3. In addition, small residential areas could be characterized by a more accurate management and by a

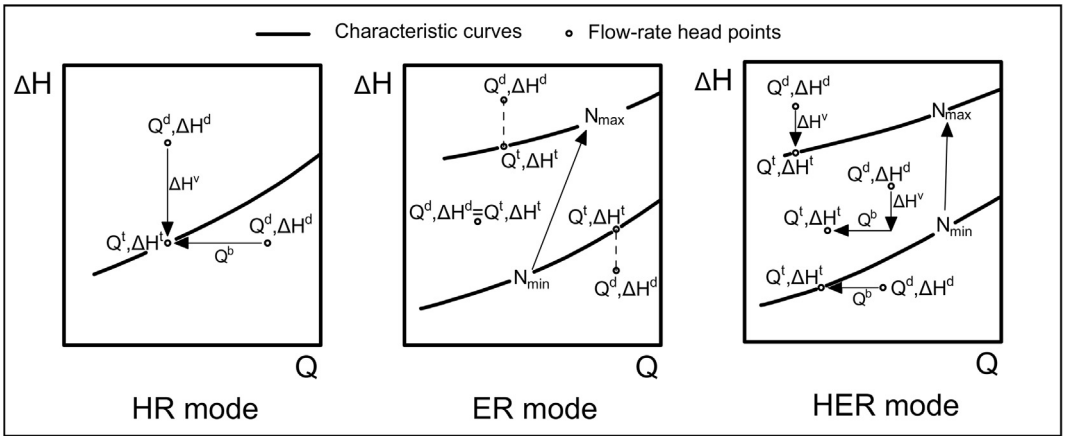

Fig. 2. –Different types of PAT regulation system: Hydraulic mode (HR), Electrical mode (ER) and Hydraulic and Electric mode (HER).

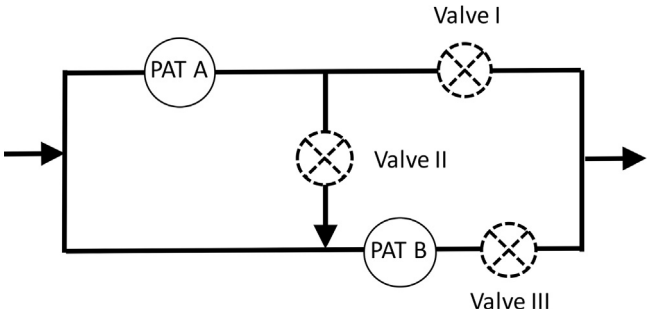

Fig. 3. New PAT regulation based on the SSP mode.

reduced pipe leakage during the night with a flow rate approaching null values. Due to the increase in the peak demand coefficient and the potential reduction in the night demand, a HPP at the inlet of a small residential area must face a larger range of flow rates when compared to a wider water network, where the flow rate compensation tends to have a well-defined and more uniform flow pattern. As an effect of pipe friction, in the WDN, as well as in the internal network of the residential area, the available head decreases with the increasing flow rate. Therefore, for the same flow rate, the available head for energy recovery can be different, depending on the pipe material, length and diameter.

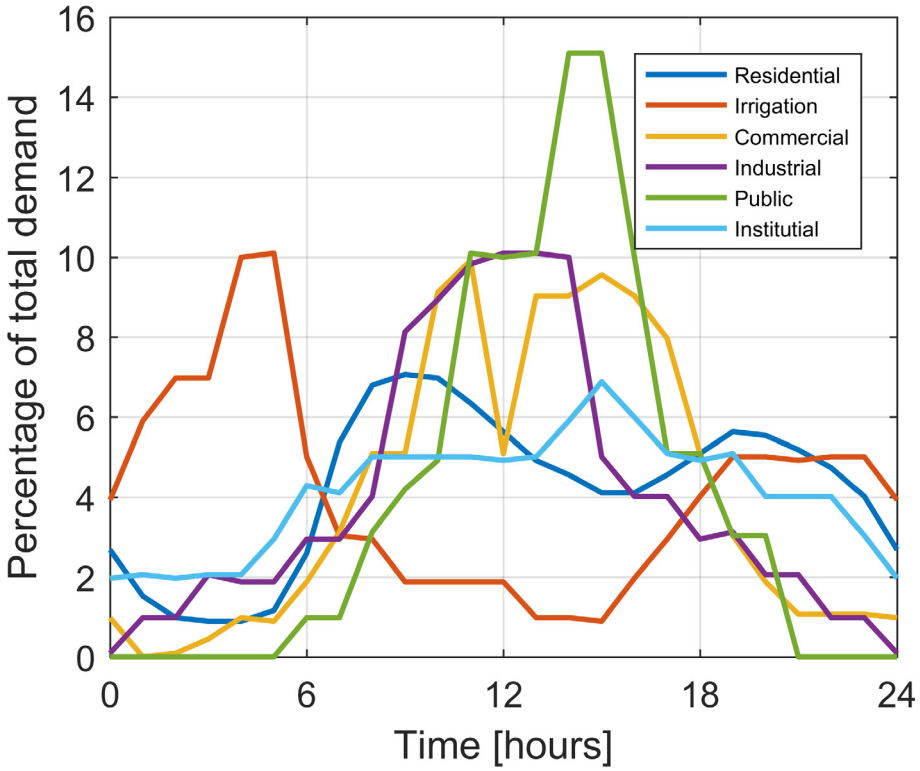

Fig. 4. Water demand for different categories in a working day.

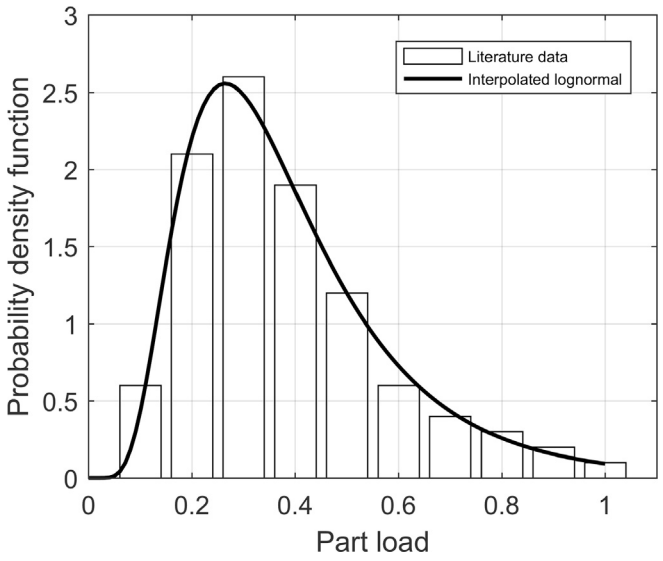

Fig. 5. Frequency distribution function of the part load of offices and hospitals, as proposed in DIN 1988.

3. Experimental investigation of the PAT behaviour

Although many semi-analytical, empirical or numerical models have recently been developed to predict the performance of a PAT operating as a turbine [16,41–43], experimental tests allow the obtainment of reliable data relating to the behaviour of the PAT [17,44]. Experiments were performed in the laboratory of Hydraulics at the Instituto Superior Técnico of the University of Lisbon, on a centrifugal Pentax water pump working as a PAT. A schematic view of the experimental facility is shown in Fig. 6.

The main working data of the pump are the following:

Flow rate: $Q = 13–210\ \mathrm{l\ min^{-1}}$
Maximum head jump: $\Delta H_{max} = 47$ m.
Head jump range: $\Delta H = 7–45$ m.
Rotational speed: $N_R = 2850$ r. p.m.
Runner diameter: D = 160 mm.
Target BEP flow rate: $Q_R = 2{,}5\ \mathrm{l\ s^{-1}}$
Target BEP head drop: $H_R = 30$ m.
BEP efficiency: $\eta = 50\%$
Specific speed: Ns = 11 r. p.m (m, $\mathrm{m^3 s^{-1}}$).

The tests performed (approximately 70 in total) consisted in the measurement of the flow rate (Q), net head (H), rotational speed (N) and torque (B) relating to the PAT under analysis, with a low value of Ns. All the experiments were performed according to the protocol detailed in UNI-EN ISO 9906.

This type of PAT seems to be that best suited to the real conditions of medium heads and low flow rates, which may be available in small residential supply systems. A turbine converts the hydraulic power, P_H, of the stream flowing through the turbine blades into mechanical power, P_{MEC}, available at the turbine shaft. The hydraulic power is a function of the discharge, Q, and head drop, ΔH, while the mechanical power is calculated as the product of the torque, B, and rotational speed, N. The efficiency of the PAT can be defined as the ratio between the mechanical power produced and the input hydraulic power, as follows:

$$P_H = \gamma Q \Delta H \tag{1}$$

$$P_{MEC} = BN \tag{2}$$

$$\eta = \frac{P_{MEC}}{P_H} \tag{3}$$

γ being the specific weight of the water. The experiments were conducted on flow values between 2.0 l/s and 4.6 l/s, while the available pressure head ranged between 7.0 m and 27.5 m. The characteristic and efficiency curves in inverse mode were found experimentally, for a rotational PAT speed N varying in the range 1800–3200 rpm. The flow rate was measured with a signet 8550 flow transmitter (±0.5% of reading) and calibrated with a triangular weir (±0.5% of reading). The pressure at the PAT inlet and outlet was measured with WIKA S10pressure transducers (±0.1% accuracy). The PAT rotational speed was measured with a ST-723 digital optical tachometer ±0.1% accuracy). The mechanical torque at the PAT axis was measured with a torque break (±0.1% accuracy).

Fig. 7 shows the performance power and headcurves in dimensionless units φ, χ, ψ, defined as follows:

$$\phi = \frac{Q}{ND^3}, \chi = \frac{g\Delta H}{N^2D^2}, \psi = \frac{P_{MEC}}{\rho N^3 D^5} \tag{4}$$

Despite the high accuracy of the measuring instruments, the theory of the propagation of errors demonstrates that the error in the measurement of the efficiency amplifies. All the measurements complied with the UNI EN ISO 9906 - level b standards for performance tests on turbomachines. Thus, the extended uncertainty on the evaluation of the efficiency, δ_η, can be evaluated as [45]:

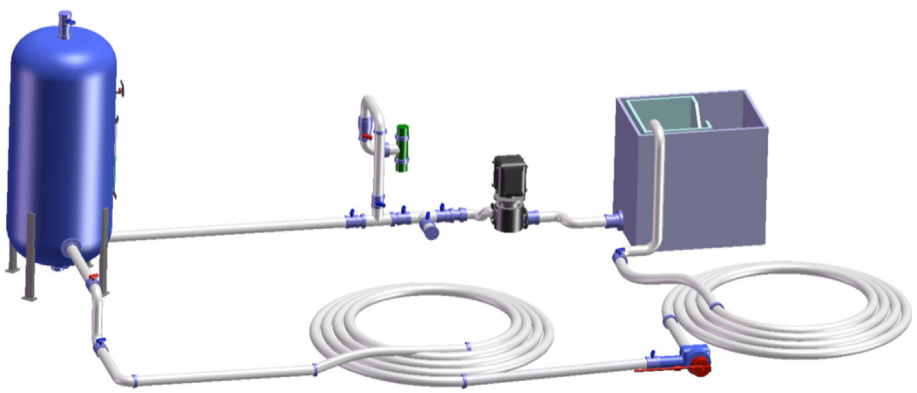

Fig. 6. Photo of the PAT experimental set-up with upstream pressure regulation and downstream flow rate measurement.

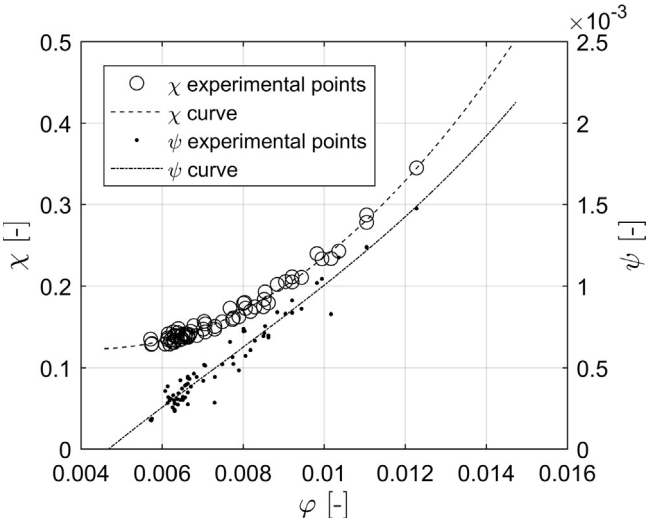

Fig. 7. Characteristic curves for the PAT tested in the laboratory.

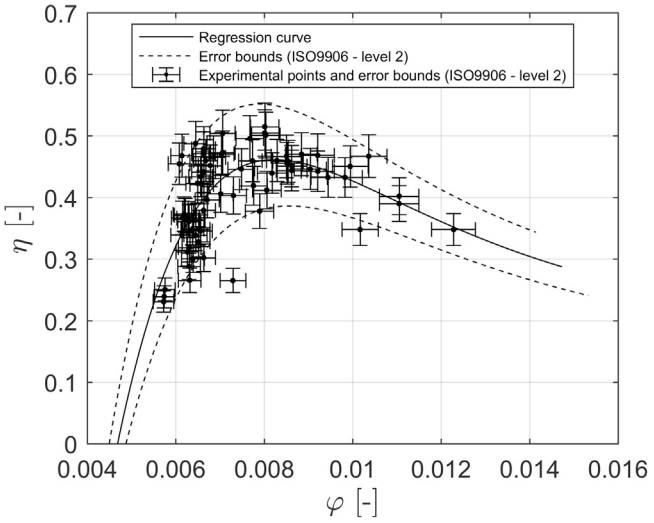

Fig. 8. Efficiency curves for the PAT tested in the laboratory.

$$\delta_\eta = \sqrt{\delta_H^2 + \delta_B^2 + \delta_N^2 + \delta_Q^2} \tag{5}$$

while the uncertainties on the measurements of φ, χ and ψ, δ_ϕ, δ_χ and δ_ψ respectively, can be calculated as:

$$\begin{aligned} \delta_\phi &= \sqrt{\delta_N^2 + \delta_Q^2} \\ \delta_\chi &= \sqrt{\delta_H^2 + 2\delta_N^2} \\ \delta_\psi &= \sqrt{\delta_B^2 + 2\delta_N^2} \end{aligned} \tag{6}$$

where δ_H, δ_B, δ_N and δ_Q are the extended uncertainties on the measurements of the head, torque, rotational speed and discharge respectively. According to the UNI EN ISO 9906 - level b standards, $\delta_H = \mp 5.5\%$, $\delta_B = \mp 3\%$, $\delta_N = \mp 2\%$ and $\delta_Q = \mp 3.5\%$. Thus, δ_η can be calculated as $\mp 6.1\%$.

In order to evaluate the dependency of η on ϕ, two regression curves $\chi = \chi(\varphi)$ and $\psi = \psi(\varphi)$ were used to obtain the efficiency regression curve, whose expression can be obtained as follows:

$$\eta(\phi) = \frac{\psi(\phi)}{\phi \cdot \chi(\phi)} \tag{7}$$

In Fig. 7, the experimental points of the efficiency are shown together with their own error bounds. Furthermore, the regression curve obtained by equation (5), together with its error bounds, is plotted. The figure shows that most of the experimental points are contained within the uncertainty region of the efficiency, demonstrating the compliance between the experimental measurements and the UNI EN ISO9906 level b standards. The influence of the choice of the efficiency regression curve among the three curves of Fig. 8 is shown hereafter, to demonstrate the impact of the error in the estimation of the efficiency.

4. The new PAT regulation mode

The new single-serial-parallel regulation (SSP) mode has been introduced to reduce the cost of the side equipment necessary for plant regulation: valves, an inverter and a control unit. The installation scheme is reported in Fig. 3. Three on/off valves and two identical PATs are used to obtain three different HPP working conditions:

a) Valve I on, PAT A on, valve II and valve III Off, PAT B off – single PAT;
b) Valve II and valve III on, PAT A and PAT B on, valve I off – series PATs;
c) Valve I and valve III on, PAT A and PAT B on, valve II off – parallel PATs.

In the working condition "a", a single PAT produces energy for intermediate values of discharge; in the working condition "b", two PATs work in series when the available head is higher; finally, in the "working condition "c", the two PATs work in parallel to deal with the highest discharge demand.

An example of the working conditions of the SSP plant is plotted in Fig. 9, together with the flow rate-head curve (Q, ΔH^d). The power plant will work under working condition "a", "b" or "c". When two PATs are working in series (case "b"), the head drop deliverable by the HPP will be twice the head drop of a single PAT, for a given flow rate, and the characteristic curve is shifted upwards, when compared to a single PAT (case "a"). When two PATs are working in parallel (case "c"), each PAT will work with half of the flow rate and

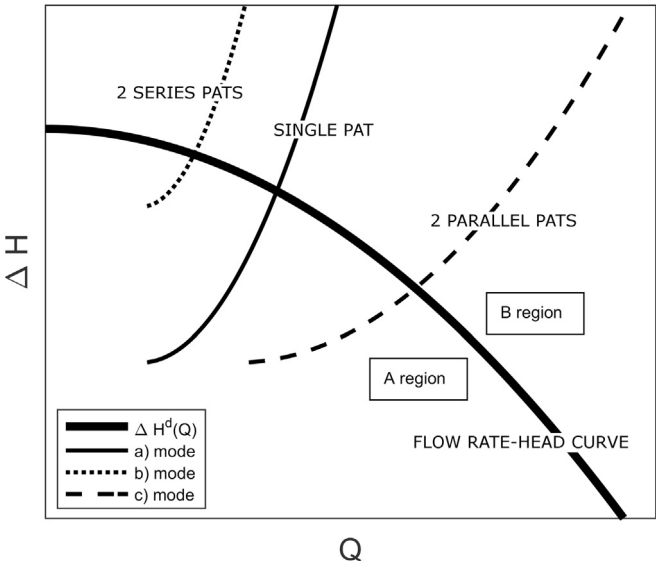

Fig. 9. Working conditions of the tested PAT, at N = 1800 rpm, in the SSP regulation mode.

the characteristic curve will be shifted horizontally, when compared to case a. Differently from the ER, HR and HER regulation schemes, in SSP the head-drop deliverable by the HPP will never match the available head (except for a few points at the intersection of the operating conditions curve and the characteristic curve). Nevertheless, the SSP scheme can be of technical interest due to its low installation costs and its simple installation and regulation, as presented below. During the operation, a smaller head drop will be obtained in the network when the ΔHT point in Fig. 9 is located in the "A" region. On the contrary, the HPP will produce a larger head drop when the ΔHT pointl is located in the "B" region.

When the power plant operates in the "A" region, some problems could arise in the water supply due to the lower backpressure values and an upper constraint must be given to limit the positive difference between ΔH^T and ΔH^d. Instead, a negative difference is acceptable, reflected in higher values of the pressure head than the required minimum.

A list of set points will be necessary to activate the valves and the PATs according to the different working conditions. For the existence of a relation between the flow rate and head drop in the network, the set points could be fixed in terms of the flow rate or pressure. The PAT geometry and set points are the results of the specific design criteria of each water system.

Finally, recent studies [20,46,47] have demonstrated that the modifications of the hydraulic behaviour of the network are very slow and the system can be modelled in a quasi-steady state. Even when an abrupt change in the discharge or head occurs, the operation of the valves of the HPP can face such a variation with little dynamic effect.

5. Design criteria

According to VOS, the PAT design solution can be found by maximizing the power plant effectiveness:

$$e = A_1 \cdot A_2 \cdot A_3 \cdot \ldots \cdot A_m \tag{8}$$

where A_1, …, A_m are m performance indicators of the system influencing its overall effectiveness e. The influence of different kinds of indicators has been discussed in previous papers [29,48].

The first indicator is the system capability, η_P^i. It can be defined as the ratio between the electrical energy produced and the hydraulically available energy for a given operating point. It can be calculated as:

$$\eta_p^i = \frac{\Delta H_i^T \Delta_i^T \eta_i^T \Delta t_i}{\Delta H_i^d Q_i^d \Delta t_i} \tag{9}$$

The second indicator is the PAT reliability, μ_P^i. Reliability is the probability that a component, system or process will work without failure for a specified duration when operated correctly under specified conditions [49]. The probability of failure of an engineering system is often represented by an exponential probability distribution [50]:

$$R(t) = e^{-\lambda t} \tag{10}$$

where λ is the failure rate, equal to 1/MTTF, namely, the mean time to failure [51].

When a pump is operating away from its BEP, its reliability decreases [52,53]. The reliability μ_P^i can be expressed as the ratio between the MTTF at a flow discharge away from the BEP and the MTTF at the BEP [29], as the following:

$$\mu_P^i = \frac{MTTF\left(Q_i^T / Q_{BEP}\right)}{MTTF(Q_{BEP})} \tag{11}$$

For industrial pumps, based on the manufacturer's experience of the resistance of machine components according to the ANSI standards, the reliability curve is given in Fig. 10. This curve has recently been modified for PATs, considering the different loads of a pump working in inverse mode, as plotted in the same figure.

The third parameter is the plant sustainability, χ_P^i. In the SSP regulation mode, the deliverable head drop could be significantly different from the available head drop, due to the difference between the network discharge-head point and the characteristic curve, Fig. 10. A penalty should be considered in the optimization process and such a penalty can be included as a factor in the calculation of the effectiveness. This new factor, namely the plant sustainability, χ_P, ranges between 0 and 1 and has been defined as:

$$\chi_P^i = \left(1 + \alpha \frac{\left|\Delta H_i^T - \Delta H_i^d\right|}{BP}\right)^{-1} \tag{12}$$

where α is a coefficient influencing the decay of effectiveness when the net head produced is different from the design value, and BP is the backpressure required value. In this work, α has been set to 10, and therefore an error equal to 10% in the backpressure halves the effectiveness of the plant.

Thus, the effectiveness, is defined as:

$$e^i = \eta_P^i \cdot \mu_P^i \cdot \chi_P^i \tag{13}$$

Therefore, in the optimization procedure, the objective function is defined, for each operating point, as:

$$e^i = max\left[e_i^a,\ e_i^b, e_i^c\right] \tag{14}$$

The overall effectiveness of the plant can be expressed as:

$$\mathrm{e} = \frac{1}{n} \sum_{i=1}^{n} e^i \tag{15}$$

where n is the number of the operating points considered for the plant design and e_i^a, e_i^b and e_i^c are the calculated effectiveness of the i-th operating point with the HPP working in mode a), b), or c), respectively. In the SSP mode the power plant is assumed to work at

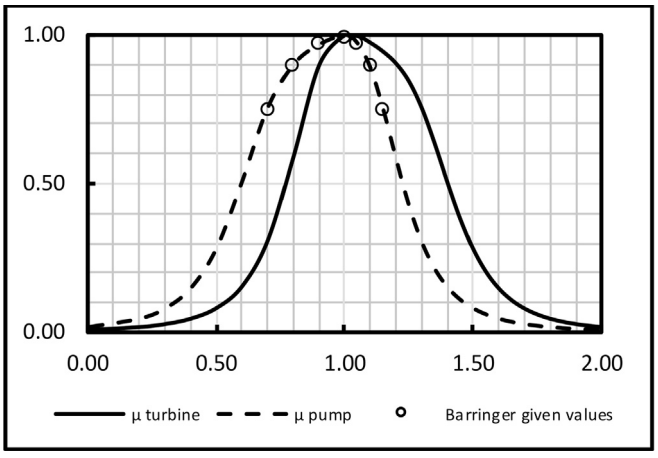

Fig. 10. Standard reliability curves for pump and turbine modes.

any operating point with the maximum effectiveness. Consequently, the optimization procedure generates automatically the values of the set point necessary to activate the valves and the PATs according to the different operating modes.

In conclusion, the design parameters were obtained with the following procedure:

1. A set of operating conditions (Q^d_i, ΔH^d_i) is given;
2. A maximum positive 5 m difference between ΔH^T and ΔH^d is accepted;
3. Dimensionless PAT working curves, experimentally determined, are used
4. For each operating point, the objective function is calculated by equation (13);
5. The highest value of effectiveness is chosen (14) for each operating point and the corresponding working condition is accordingly selected;
6. The overall plant effectiveness is calculated by equation (15):

6. Results

The fine-tuning of the operation of the plant was performed with reference to several machines at different rotating speeds, in order to evaluate the potential of the SSP. Several different plants were modelled with different patterns of head and discharge and several machines were simulated, based on the experimental results, with the application of the affinity law [54,55] by setting different values of the impeller diameter (ranging between 80 and 240 mm) and rotational speed (from 1200 to 3200 rpm). For the centrifugal pump used for the testing, according to the dimensionless PAT characteristic and efficiency curves, the range of variation of the BEP flow rate was 1.8 l/s (N = 1200 rpm, D = 120 mm) and 11.3 l/s (N = 3200 rpm, D = 160 mm), with a corresponding head drop of 4.1 m and 51.6 m.

The performances of all the simulated machines were tested on different patterns of discharge and head, to simulate the different locations of the HPP in the network, with Q_{load}/Q_{BEP} and H_0/H_{BEP} varying in the range 1–10, Q_{load} being the peak flow rate and H_0 the static head drop. The values of the flow rates for each 15 min for four weeks (2688 values) were randomly extracted based on the lognormal distribution of Fig. 5 using the Monte Carlo technique. The available head was calculated based on a quadratic relation between the friction losses and flow rate.

Table 1 shows, for each rotational speed, the best values of the runner diameter, Q_{load}/Q_{BEP} and H_0/H_{BEP}, i.e. the values of the parameters which produce the greatest effectiveness. All solutions present values of Q_{load}/Q_{BEP} and H_0/H_{BEP} that can be considered very close (ranging respectively between 3.1 and 3.4 and between 1.7 and 1.9). Given the peak flow rate (Q_{load}) and the static pressure head (H_0) at the power plant location, the design parameters Q_{BEP} and H_{BEP} are identified. Effectiveness values were found to vary slightly up to 2300 rpm and to reduce for increasing runner speeds. In the last column of Table 1, the HPP capability, η_P (calculated as the ratio of the total produced energy and the total available energy), is reported. It is stable at around 20%. Since the plant capability and the plant effectiveness are obtained by the sum of 2688 values – see equation (13) – the effect of the propagation of the experimental errors becomes negligible, since the algebraic sum reduces the propagated error [45]. The last four columns of Table 1 show the values of effectiveness and plant capability when the efficiency curve is overestimated (e^-, η_p^-) or underestimated (e^+, η_p^+). The two bound regression curves of Fig. 8 were used in the calculations. The impact of the error in the estimation of the machine efficiency is lower by about 4% in terms of plant capability and by about 2% in terms of plant effectiveness.

The results for N = 1200 rpm and D = 140 mm are discussed herein. The greatest effectiveness was obtained for $Q_{load}/Q_{BEP} = 3.4$ and $H_0/H_{BEP} = 1.8$ (e = 10.65%). The monthly energy production was 56.36 kWh, representing 20.88% of the available energy.

In Fig. 11, the effectiveness is plotted versus H_0/H_{BEP}, for different Q_{load}/Q_{BEP} ratios. The PAT performance seems very sensitive to any variation in either ratio, and the effectiveness decreases quite fast when the Q_{load}/Q_{BEP} and H_0/H_{BEP} values move far from the best design solution.

In Fig. 12, the energy produced is plotted versus H_0/H_{BEP}, for different Q_{load}/Q_{BEP} ratios. The energy produced increases for increasing values of H_0/H_{BEP} because an increase in the available head generates an increase in the energy produced. For large H_0/H_{BEP} values the power plant works for flow rates and a head drop far from the PAT best efficiency values and the plant reliability collapses. The energy produced exhibits a limited variability with Q_{load}/Q_{BEP}. Hence, the power plant capability is only marginally influenced by the Q_{load}/Q_{BEP} variation.

The contribution of each working condition (single, serial or parallel) to the total HPP energy production is shown in the plot of Fig. 13 as a function of H_0/H_{BEP} for $Q_{load}/Q_{BEP} = 3.4$. For the best design solution, corresponding to $H_0/H_{BEP} = 1.8$, all working conditions contribute appreciably to the total production.

The working conditions for the best design solution with N = 1200 rpm and D = 140 mm ($Q_{load}/Q_{BEP} = 3.4$, $H_0/H_{BEP} = 1.8$) are plotted in Fig. 14, together with a number of network flow rate-head points. The set points of each working condition, as obtained by optimization, were found to be extremely regular, allowing a reliable control of the new SSP mode, based on simple pipe pressure or discharge measurements.

7. Economic and financial feasibility

The economic feasibility of a HPP should be based on the calculation of the Net Present Value (NPV) of the design solution. A similar analysis has already been performed on larger plants installed along the branches of a water supply network [18]. A HR plant, with an installed power ranging between 0.35 kW and 4.7 kW, exhibits a plant capability, η_P, ranging between 0.35 and 0.42 respectively [30], with positive values of NPV for a HR plant.

A comparison between the benefits of a HPP for a small residential area in SSP regulation or in HR regulation has been performed herein. Different load conditions have been considered, for five ranges of Q_{load} and five ranges of H_0. Next, for each combination of discharge and head the best solution, i.e. the diameter and the rotational speed which maximize the plant effectiveness, has been found. Finally, for each plant, the NPV has been estimated and compared with the NPV of the corresponding HR plant.

The NPV of the two design solutions is given by:

$$NPV = V_r - I + \sum_{j=1}^{y} \frac{R_j}{(1+r)^j} \tag{16}$$

where R_j is the net cash flow during the j-th year, y is the considered number of years, I is the starting investment, r the discount rate and V_r is the residual value of the plant after the base period considered.

The cash flow, which determines the NPV, depends both on the cost of the equipment, which results in the I value, and on the electricity selling price which produces the cash inflow during the life of the plant. In this study, a period of twenty years is considered as the base period for the assessment of the NPV, since it can be considered a reasonable period for the evaluation of the energy

Table 1
Best design solutions in the SSP regulation.

N (rpm)	D (mm)	Q_{load}/Q_{BEP} (−)	H_0/H_{BEP} (−)	E (%)	η_p (%)	e^- (%)	η_p^- (%)	e^+ (%)	η_p^+ (%)
1200	140	3.4	1.8	10.65	20.88	8.89	17.56	12.64	24.58
1300	140	3.3	1.8	10.67	20.76	8.90	17.46	12.70	24.64
1400	120	3.4	1.9	10.59	21.10	8.86	17.75	12.55	24.93
1500	120	3.5	1.8	10.66	20.84	8.89	17.54	12.65	24.38
1600	120	3.3	1.8	10.60	20.94	8.82	17.54	12.61	24.78
1700	120	3.3	1.8	10.46	20.76	8.71	17.48	12.44	24.52
1800	100	3.4	1.9	10.50	21.16	8.78	17.76	12.46	25.07
1900	100	3.4	1.9	10.55	21.08	8.82	17.77	12.49	24.95
2000	80	3.4	1.7	10.56	19.78	8.82	16.67	12.56	23.41
2100	80	3.4	1.7	10.65	20.24	8.87	16.99	12.68	23.91
2200	80	3.4	1.7	10.68	20.36	8.88	17.18	12.72	24.05
2300	80	3.4	1.7	10.67	20.50	8.87	17.29	12.71	24.11
2400	80	3.3	1.7	10.61	20.52	8.79	17.22	12.67	24.32
2500	80	3.3	1.7	10.53	20.60	8.72	17.29	12.58	24.39
2600	80	3.3	1.7	10.42	20.60	8.62	17.30	12.44	24.31
2700	80	3.2	1.7	10.25	20.65	8.46	17.25	12.30	24.61
2800	80	3.2	1.7	10.09	20.65	8.31	17.21	12.10	24.55
2900	80	3.2	1.7	9.93	20.63	8.17	17.24	11.91	24.50
3000	80	3.3	1.7	9.75	20.32	8.03	17.02	11.67	24.03
3100	80	3.3	1.7	9.54	20.14	7.85	16.94	11.45	24.02
3200	80	3.1	1.7	9.34	20.64	7.64	17.06	11.23	24.69

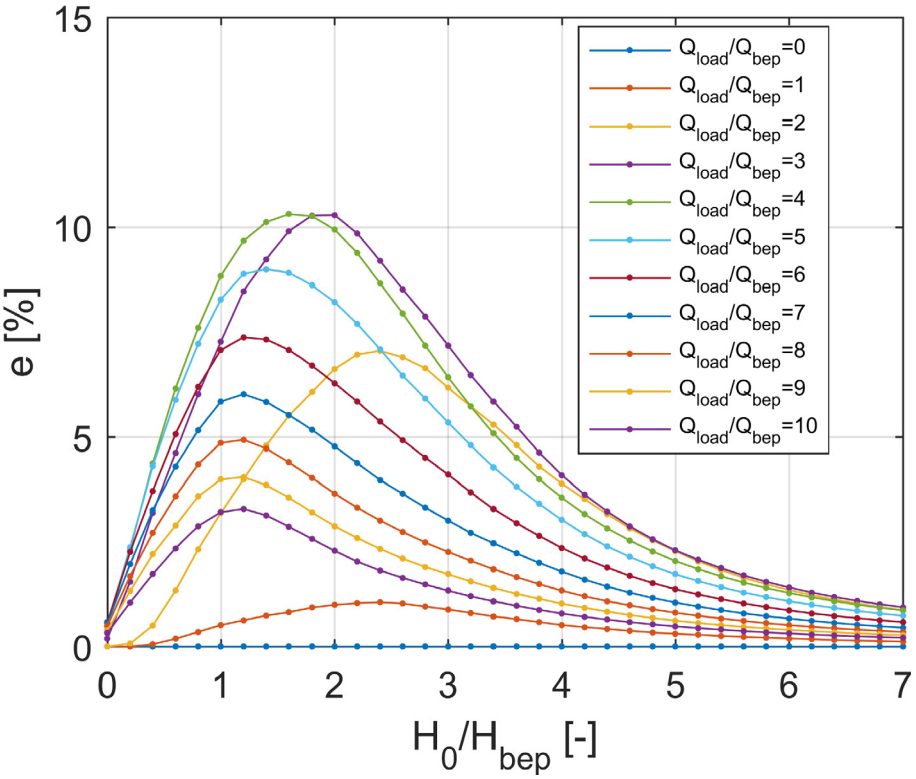

Fig. 11. The effectiveness of the SSP plant with N = 1200 rpm, D = 140 mm for different rations of Ho/$H_{BEP}$and Q_{load}/Q_{BEP}.

investment of a water company. Thus, both the residual value and the maintenance costs can be discounted with a satisfactory approximation. The energy price depends on the country. Due to the presence of feed-in tariffs in southern Italy energy tariffs can be as high as 0.22€/kWh. The twenty years government bond rate for Italy was assumed equal to 0.01.

The total plant cost in HR has been evaluated as €15,500, while a provisional plant cost in SSP is €4450. A detailed description of the costs is reported in Table 2. In Table 3, for different load situations, i.e. for different ranges of Q_{load} and H_0, the optimal rotational speed and the optimal impeller diameter are shown, together with the effectiveness, capability, monthly produced energy (E) and compared values of NPV^{SSP} and NPV^{HR}, i.e. the estimated net present values of the SSP plant and HR plant respectively.

In terms of NPV, the two plants behave differently. The NPV^{SSP} is often greater than the NPV^{HR}. Indeed, despite the lower efficiency (about 20% for the SSP against 35% for the HR), the cost of a SSP plant is approximately one third of the cost of a HR plant of the same size. In several cases, when the available power is very low, i.e. for the first discharge range and when the static head is low,

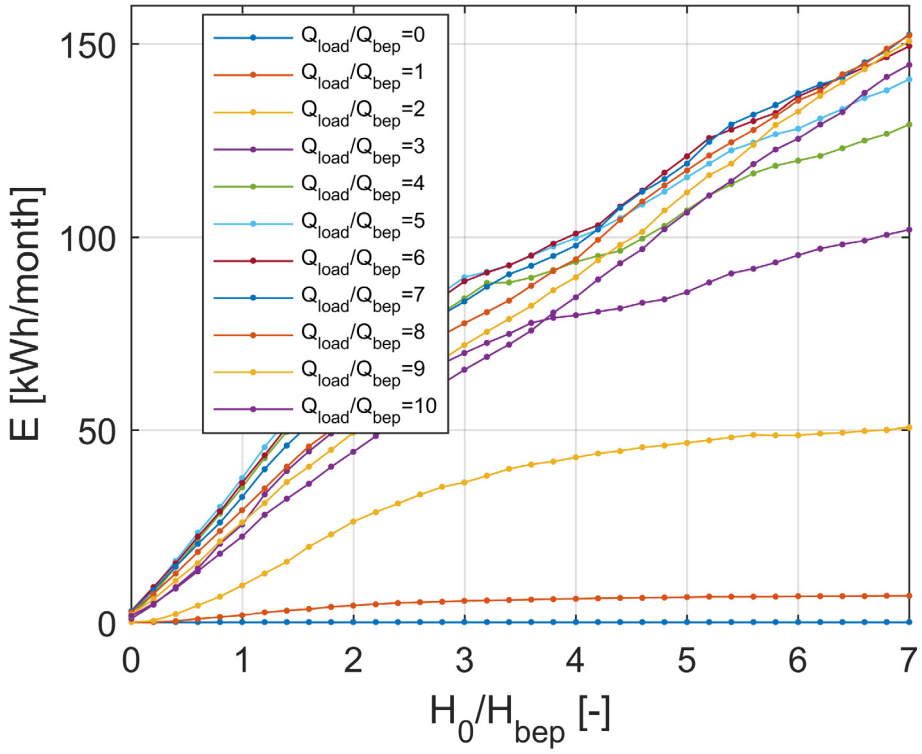

Fig. 12. The produced energy of the SSP plant with N = 1200 rpm, D = 140 mm for different rations of Ho/H_{BEP} and Q_{load}/Q_{BEP}.

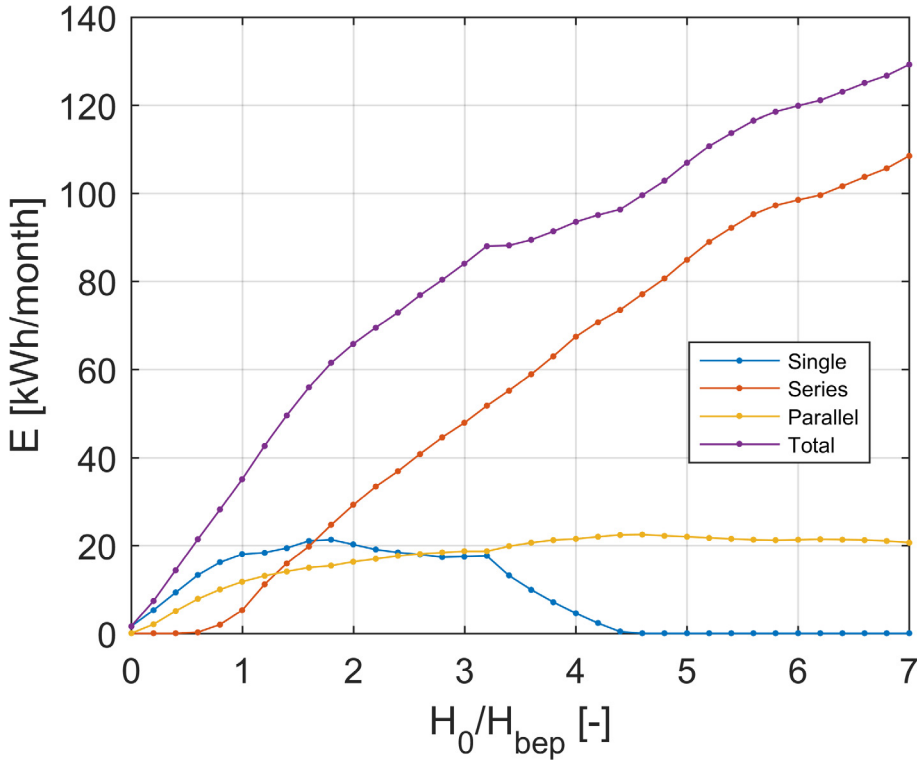

Fig. 13. The contribution of Single ("a"), Series ("b") and Parallel ("c") working conditions to the energy production of the SSP plant for $Q_{load}/Q_{BEP} = 3.4$ and different ratios of Ho/H_{BEP}.

neither of the plants is financially advantageous, since after twenty years the NPV is still negative. As the available power increases, the SSP plant is advantageous, since it exhibits positive NPV values greater than the NPV^{HR}. Then, for the largest plants (the last row of Table 3) the HR plant is more advantageous than the SSP plant. Therefore, SSP seems the only viable solution to obtain energy

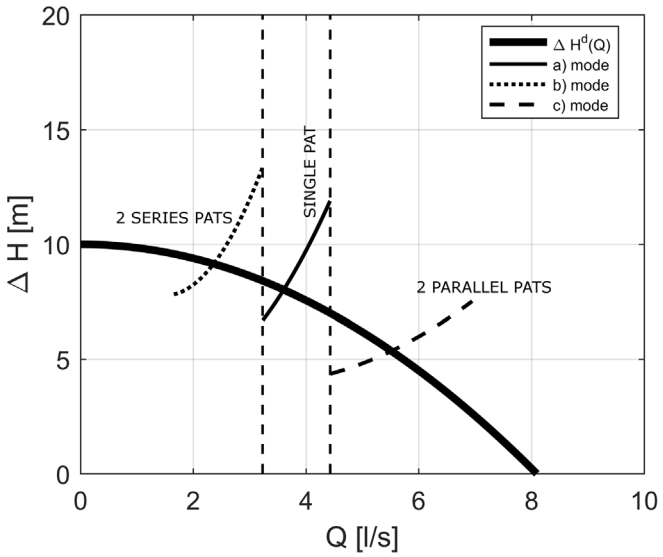

Fig. 14. The working conditions of the SSP plant in Series ("a"), Single ("b") and Parallel ("c") working conditions compared with the network available points for N = 1200 rpm, D = 140 mm, $Q_{load}/Q_{BEP} = 3.4$ and $Ho/H_{BEP} = 1.8$.

recovery in the peripheral areas of water networks or in small residential areas.

Finally, the levelized cost of energy (LCOE) has been evaluated for the SSP plant, as reported in the last column of Table 3. The LCOE can be calculated as [56]:

$$\mathrm{LCOE} = \frac{I + \sum_{j=1}^{life} \frac{C_m}{(1+r)^j}}{\sum_{j=1}^{life} \frac{E_j}{(1+r)^j}} \tag{16}$$

where C_m is the yearly maintenance cost, and E_j is the yearly energy production with the life of the system set at 30 years. According to several studies, the sum of the maintenance costs during the whole lifetime of a pumping system is comparable to the initial investment [57,58] and has been set at 4550 € herein. The resulting values of the LCOE are comparable to the alternative renewables – for example, the LCOE of solar photovoltaic energy can be assessed as 0.05–0.5 €/kWh - [59,60], demonstrating the feasibility of the SSP plant.

8. Conclusions

In the peripheral areas of water supply networks, a largely

Table 2
Economic details of HR and SSP plants.

	HR plant		SSP plant	
Plant cost [€]	Pump	700	Pumps	1400
	2 control valves	14400	3 on-off valves	2100
	Grid connection	200	PLC controller	500
	Piping	200	2 pressure transducers	50
			Grid connection	200
			Piping	200
	TOTAL	15500	TOTAL	4450

Table 3
Optimal plant design for several load situations and estimated NPVs.

Q_{load}	H_0	N	D	e^{ott}	η^{ott}	E	NPV^{SSP}	NPV^{hr}	LCOE
		rpm	mm	%	%	kwh/month	€	€	€/kWh
$0<Q_{load}<4$	$0 < H_0 < 10$	2100	80	10.65	20.24	19.23	−3534	−13915	1.49
$0<Q_{load}<4$	$10 < H_0 < 20$	2200	80	10.68	20.36	21.42	−3430	−13746	1.34
$0<Q_{load}<4$	$20 < H_0 < 30$	2900	80	9.61	20.77	44.05	−2351	−11963	0.65
$0<Q_{load}<4$	$30 < H_0 < 40$	3200	80	6.80	20.89	67.16	−1250	−10138	0.43
$0<Q_{load}<4$	$40 < H_0 < 50$	3000	100	3.02	13.94	57.87	−1693	−8576	0.50
$4<Q_{load}<8$	$0 < H_0 < 10$	1400	120	10.45	20.27	39.45	−2570	−12255	0.73
$4<Q_{load}<8$	$10 < H_0 < 20$	1500	120	10.66	20.84	49.32	−2100	−11553	0.58
$4<Q_{load}<8$	$20 < H_0 < 30$	2400	100	9.71	20.73	70.26	−1103	−9849	0.41
$4<Q_{load}<8$	$30 < H_0 < 40$	3000	100	8.18	20.27	121.33	1330	−5517	0.24
$4<Q_{load}<8$	$40 < H_0 < 50$	3200	100	6.80	21.23	156.41	3001	−3217	0.18
$8<Q_{load}<12$	$0 < H_0 < 10$	1200	140	10.58	20.76	55.21	−1820	−11065	0.52
$8<Q_{load}<12$	$10 < H_0 < 20$	1300	140	10.67	20.76	68.60	−1182	−9989	0.42
$8<Q_{load}<12$	$20 < H_0 < 30$	2000	120	9.65	20.41	108.74	730	−6616	0.26
$8<Q_{load}<12$	$30 < H_0 < 40$	2900	100	8.25	20.28	131.19	1800	−4714	0.22
$8<Q_{load}<12$	$40 < H_0 < 50$	3200	100	7.10	19.93	190.22	4612	411	0.15
$12<Q_{load}<16$	$0 < H_0 < 10$	1300	140	10.34	18.66	64.14	−1394	−9769	0.45
$12<Q_{load}<16$	$10 < H_0 < 20$	1200	160	10.61	20.56	103.13	463	−7135	0.28
$12<Q_{load}<16$	$20 < H_0 < 30$	1700	140	9.63	20.64	141.25	2279	−4089	0.20
$12<Q_{load}<16$	$30 < H_0 < 40$	2100	140	8.20	19.97	265.40	8194	6661	0.11
$12<Q_{load}<16$	$40 < H_0 < 50$	2800	120	7.24	19.93	274.67	8635	7482	0.10
$16<Q_{load}<20$	$0 < H_0 < 10$	1200	160	10.26	17.83	86.60	−324	−7403	0.33
$16<Q_{load}<20$	$10 < H_0 < 20$	1200	160	10.34	18.70	99.11	272	−6661	0.29
$16<Q_{load}<20$	$20 < H_0 < 30$	1500	160	9.51	20.50	193.14	4751	209	0.15
$16<Q_{load}<20$	$30 < H_0 < 40$	2100	140	8.09	19.70	270.56	8439	7401	0.11
$16<Q_{load}<20$	$40 < H0<50$	2400	140	7.19	19.92	380.15	13660	16326	0.08

unexploited excess energy is often present, for pressure values greater than the minimum required pressure. According to the modern trend for a sustainable management of natural resources, this energy should be recovered. However, the low values of available power and the large variations of flow rate and pressure drop, and the consequent need for an expensive power plant control system, hinder the diffusion of such a practice for small residential areas.

In this paper, a new control system for a HPP using a PAT for energy recovery is discussed. The new technical solution is based on a relaxation of the pressure constraint and on a simplified regulation mode, the Single-Serial-Parallel (SSP) scheme. Two PATs are piped with three on-off valves to obtain three working conditions: single, series and parallel modes, respectively. The power plant working condition adapts to the water network working condition by switching from one mode to another when the pressure drop decreases.

An appropriate design strategy has been developed for SSP regulation, based on maximizing the power plant effectiveness for each network operating condition. Based on experimental results on a centrifugal pump working in inverse mode, different machines have been modelled with the application of the turbomachinery affinity law. Different load conditions, (i.e different values of maximum discharge and static head) have been simulated, based on the frequency distribution of the discharge in a small residential area. The design results, obtained by the maximization of the effectiveness of the plant, are presented in a dimensionless form to allow an easy extension of the results to different network flow parameters.

A power plant capability, as defined by equation (9), approximately equal to 20% has been obtained. This value is apparently much lower than 35%, which is the capability value obtained in the classic PAT hydraulic regulation mode for a similar plant size. However, with SSP, the cost of the newly proposed SSP plant reduces to one third. The calculation of the levelized cost of energy demonstrates that the proposed SSP plant can be considered an interesting investment aimed at the production of renewable energy, when compared to other energy sources. Indeed, the economic assessment has demonstrated that the proposed plant is more profitable than other hydro installation schemes, when the available power is low, due to its lower installation costs. With reference to the several analysed load conditions, it can be considered an interesting investment if the available power is not too low, i.e. when more than about 100 kWh/month can be produced. Conversely, as the produced energy increases, its economic feasibility decreases Other solutions should be preferred if the power produced is greater than 380 kWh/month, a decision related to the lower capability of the plant when compared to traditional hydropower plants.

List of symbols

C_m	yearly maintenance cost
E_j	energy production at the j-th year
P_H	hydraulic power
P_{MEC}	mechanical power
R_j	revenue at the j-th year
V_r	residual value of the plant
δ_f	uncertainty of the measurement of f
η_P	capability of the plant
μ_P	reliability of the plant
χ_P	sustainability of the plant
LCOE	levelized cost of energy
NPV	net present value
ΔH	head jump
B	Torque
BP	backpressure
D	diameter of the impeller of the PAT
I	investment cost
$MTTF$	mean time to failure
N	rotational speed of the PAT
Q	discharge
$R(t)$	probability of failure after t time
e	effectiveness
g	gravity acceleration
r	discount rate
γ	specific weight of water
η	efficiency
λ	failure rate
ρ	density of water
ϕ	dimensionless discharge
χ	dimensionless head drop
ψ	dimensionless power

References

[1] T. Walski, W. Bezts, E. Posluzny, M. Weir, B. Whitman, Modelling leakage reduction through pressure control, J. Am. Water Work Assoc. 98 (2006) 147–152.

[2] K. Vairavamoorthy, J. Lumbers, Leakage reduction in water distribution systems: optimal valve control, J. Hydraul. Eng. 124 (1998) 1146–1154, https://doi.org/10.1061/(ASCE)0733-9429(1998)124:11(1146).

[3] T. Tucciarelli, A. Criminisi, D. Termini, Leak analysis in pipeline systems by means of optimal valve regulation, J. Hydraul. Eng. 125 (1999) 277–285, https://doi.org/10.1061/(ASCE)0733-9429(1999)125:3(277).

[4] L. Araujo, H. Ramos, S. Coelho, Pressure control for leakage minimisation inWater distribution systems management, water resour, Manag 20 (2006) 133–149, https://doi.org/10.1007/s11269-006-4635-3.

[5] M. Nicolini, L. Zovatto, Optimal location and control of pressure reducing valves in water networks, J. Water Resour. Plan. Manag. 135 (2009) 178–187, https://doi.org/10.1061/(ASCE)0733-9496(2009)135:3(178).

[6] L.F.R. Reis, R.M. Porto, F.H. Chaudhry, Optimal location of control valves in pipe networks by genetic algorithm, J. Water Resour. Plan. Manag. 123 (1997) 317–326, https://doi.org/10.1061/(ASCE)0733-9496(1997)123:6(317).

[7] A. Dannier, A. Del Pizzo, M. Giugni, N. Fontana, G. Marini, D. Proto, Efficiency evaluation of a micro-generation system for energy recovery in water distribution networks, in: 2015 Int. Conf. Clean. Electr. Power, 2015, pp. 689–694, https://doi.org/10.1109/ICCEP.2015.7177566.

[8] A. Carravetta, L. Antipodi, U. Golia, O. Fecarotta, Energy saving in a water supply network by coupling a pump and a Pump as Turbine (PAT) in a turbopump, WaterSwitzerl. 9 (2017), https://doi.org/10.3390/w9010062.

[9] H.M. Ramos, M. Mello, P.K. De, Clean power in water supply systems as a sustainable solution: from planning to practical implementation, Water Sci. Technol. Water Supply 10 (2010) 39, https://doi.org/10.2166/ws.2010.720.

[10] A. McNabola, P. Coughlan, L. Corcoran, C. Power, A.P. Williams, I. Harris, J. Gallagher, D. Styles, Energy recovery in the water industry using micro-hydropower: an opportunity to improve sustainability, Water Policy 16 (2014) 168–183, https://doi.org/10.2166/wp.2013.164.

[11] J. Gallagher, D. Styles, A. McNabola, A.P.P. Williams, Life cycle environmental balance and greenhouse gas mitigation potential of micro-hydropower energy recovery in the water industry, J. Clean. Prod. 99 (2015) 152–159, https://doi.org/10.1016/j.jclepro.2015.03.011.

[12] a. a. Williams, Pumps as turbines for low cost micro hydro power, Renew. Energy 9 (1996) 1227–1234, https://doi.org/10.1016/0960-1481(96)88498-9.

[13] A. Bozorgi, E. Javidpour, A. Riasi, A. Nourbakhsh, Numerical and experimental study of using axial pump as turbine in Pico hydropower plants, Renew. Energy 53 (2013) 258–264, https://doi.org/10.1016/j.renene.2012.11.016.

[14] M. Arriaga, Pump as turbine - a pico-hydro alternative in Lao People's democratic republic, Renew. Energy 35 (2010) 1109–1115, https://doi.org/10.1016/j.renene.2009.08.022.

[15] A. Carravetta, S. Derakhshan Houreh, H.M. Ramos, Pumps as Turbines, Springer, Cham, Switzerland, 2018, https://doi.org/10.1007/978-3-319-67507-7.

[16] S.S. Yang, S. Derakhshan, F.Y. Kong, Theoretical, numerical and experimental prediction of pump as turbine performance, Renew. Energy 48 (2012) 507–513, https://doi.org/10.1016/j.renene.2012.06.002.

[17] F. Pugliese, F. De Paola, N. Fontana, M. Giugni, G. Marini, Experimental characterization of two Pumps as Turbines for hydropower generation, Renew. Energy 99 (2016) 180–187, https://doi.org/10.1016/j.renene.2016.06.051.

[18] P. Kerschberger, A. Gehrer, Hydraulic development of high specific-speed pump-turbines by means of an inverse design method, numerical flow-simulation (CFD) and model testing, IOP Conf. Ser. Earth Environ. Sci. 12 (2010) 12039, https://doi.org/10.1088/1755-1315/12/1/012039.

[19] A. Rodrigues, P. Singh, A. Williams, F. Nestmann, E. Lai, Hydraulic analysis of a pump as a turbine with CFD and experimental data, in: IMechE Semin. Comput. Fluid Dyn. Fluid Mach, 2003.
[20] N. Fontana, M. Giugni, L. Glielmo, G. Marini, Real time control of a prototype for pressure regulation and energy production in water distribution networks, J. Water Resour. Plan. Manag. 142 (2016), 4016015, https://doi.org/10.1061/(ASCE)WR.1943-5452.0000651.
[21] M. De Marchis, B. Milici, R. Volpe, A. Messineo, Energy saving in water distribution network through pump as turbine generators: economic and environmental analysis, Energies 9 (2016) 877, https://doi.org/10.3390/en9110877.
[22] M. Giugni, N. Fontana, A. Ranucci, Optimal location of PRVs and turbines in water distribution systems, J. Water Resour. Plan. Manag. 140 (2014), 6014004, https://doi.org/10.1061/(ASCE)WR.1943-5452.0000418.
[23] I. Samora, M.J. Franca, A.J. Schleiss, H.M. Ramos, Simulated annealing in optimization of energy production in a water supply network, Water Resour. Manag. 30 (2016) 1533–1547, https://doi.org/10.1007/s11269-016-1238-5.
[24] L. Corcoran, A. Mcnabola, P. Coughlan, Optimization of water distribution networks for combined hydropower energy recovery and leakage reduction, J. Water Resour. Plan. Manag. 142 (2015) 1–8, https://doi.org/10.1061/(ASCE)WR.1943-5452.0000566.
[25] O. Fecarotta, A. McNabola, Optimal location of pump as turbines (PATs) in water distribution networks to recover energy and reduce leakage, Water Resour. Manag. (2017), https://doi.org/10.1007/s11269-017-1795-2.
[26] A. Carravetta, O. Fecarotta, G. Del Giudic, H. Ramos, Energy recovery in water systems by PATs: a comparisons among the different installation schemes, Procedia Eng. 70 (2014) 275–284, https://doi.org/10.1016/j.proeng.2014.02.031.
[27] A. Carravetta, O. Fecarotta, R. Martino, L. Antipodi, PAT efficiency variation with design parameters, Procedia Eng. 70 (2014) 285–291, https://doi.org/10.1016/j.proeng.2014.02.032.
[28] A. Carravetta, G. Del Giudice, O. Fecarotta, H.M. Ramos, Energy production in water distribution networks: a PAT design strategy, Water Resour. Manag. 26 (2012) 3947–3959, https://doi.org/10.1007/s11269-012-0114-1.
[29] A. Carravetta, G. Del Giudice, O. Fecarotta, H.M. Ramos, Pump as turbine (PAT) design in water distribution network by system effectiveness, WaterSwitzerl. 5 (2013) 1211–1225, https://doi.org/10.3390/w5031211.
[30] A. Carravetta, O. Fecarotta, M. Sinagra, T. Tucciarelli, Cost-benefit analysis for hydropower production in water distribution networks by a pump as turbine, J. Water Resour. Plan. Manag. 140 (2014), 4014002, https://doi.org/10.1061/(ASCE)WR.1943-5452.0000384.
[31] O. Fecarotta, C. Aricò, A. Carravetta, R. Martino, H.M. Ramos, Hydropower potential in water distribution networks: pressure control by PATs, Water Resour. Manag. 29 (2015) 699–714, https://doi.org/10.1007/s11269-014-0836-3.
[32] A.A. Lahimer, M.A. Alghoul, K. Sopian, N. Amin, N. Asim, M.I. Fadhel, Research and development aspects of pico-hydro power, Renew. Sustain. Energy Rev. 16 (2012) 5861–5878, https://doi.org/10.1016/j.rser.2012.05.001.
[33] N. Fontana, M. Giugni, D. Portolano, Losses reduction and energy production in water-distribution networks, J. Water Resour. Plan. Manag. 138 (2012) 237–244, https://doi.org/10.1061/(ASCE)WR.1943-5452.0000179.
[34] A.M.A. Haidar, M.F.M. Senan, A. Noman, T. Radman, Utilization of pico hydro generation in domestic and commercial loads, Renew. Sustain. Energy Rev. 16 (2012) 518–524, https://doi.org/10.1016/j.rser.2011.08.017.
[35] A. Carravetta, O. Fecarotta, U.M. Golia, M. La Rocca, R. Martino, R. Padulano, T. Tucciarelli, Optimization of osmotic desalination plants for water supply networks, Water Resour. Manag. 30 (2016) 3965–3978, https://doi.org/10.1007/s11269-016-1404-9.
[36] P.W. Mayer, W.B. Deoreo, E.M. Opitz, J.C. Kiefer, W.Y. Davis, B. Dziegielewski, J.O. Nelson, Residential end uses of water, Aquacr. Inc. Water Eng. Manag. (1999) 310. https://doi.org/4309b.
[37] A. Funk, W.B. DeOreo, Embedded Energy in Water Studies Study 3: End-use Water Demand Profiles, 2011. http://www.cpuc.ca.gov/PUC/energy/Energy+Efficiency/EM+and+V/Embedded+Energy+in+Water+Studies1_and_2.htm%5Cnftp://ftp.cpuc.ca.gov/gopher-data/energy efficiency/Water Studies 3/End Use Water Demand Profiles Study 3 FINAL.PDF.
[38] R. Hirschberg, Annual European Part Load Profile of Heating Pumps, Dusserdolf, 2008.
[39] A. Carravetta, M.C. Conte, L. Antipodi, Energy efficiency index for water supply systems, in: 2015 AEIT Int. Annu. Conf. AEIT, 2016, https://doi.org/10.1109/AEIT.2015.7415272.
[40] H.E. Babbitt, Sewerage and Sewage Treatment, John Wiley and Sons, Inc., New York, NY, 1922.
[41] X. Tan, A. Engeda, Performance of centrifugal pumps running in reverse as turbine: Part II- systematic specific speed and specific diameter based performance prediction, Renew. Energy 99 (2016) 188–197, https://doi.org/10.1016/j.renene.2016.06.052.
[42] X. Su, S. Huang, X. Zhang, S. Yang, Numerical research on unsteady flow rate characteristics of pump as turbine, Renew. Energy 94 (2016) 488–495, https://doi.org/10.1016/j.renene.2016.03.092.
[43] A. Carravetta, O. Fecarotta, H. Ramos, Numerical simulation on pump as turbine: mesh reliability and performance concerns, in: 3rd Int. Conf. Clean Electr. Power Renew. Energy Resour. Impact, ICCEP 2011, 2011, https://doi.org/10.1109/ICCEP.2011.6036260.
[44] D.R. Giosio, A.D. Henderson, J.M. Walker, P.A. Brandner, J.E. Sargison, P. Gautam, Design and performance evaluation of a pump-as-turbine micro-hydro test facility with incorporated inlet flow control, Renew. Energy 78 (2015) 1–6, https://doi.org/10.1016/j.renene.2014.12.027.
[45] J.R. Taylor, An introduction to error analysis: the study of uncertainties in physical measurements, Am. J. Phys. 51 (1983) 191, https://doi.org/10.1119/1.13309.
[46] L.E. Ormsbee, K.E. Lansey, Optimal control of water supply pumping systems, J. Water Resour. Plan. Manag. 120 (1994) 237–252.
[47] R.M. Males, R.M. Clark, P.J. Wehrman, W.E. Gates, Algorithm for mixing problems in water systems, J. Hydraul. Eng. 111 (1985) 206–219, https://doi.org/10.1061/(ASCE)0733-9429(1985)111:2(206).
[48] O. Fecarotta, H.M. Ramos, S. Derakhshan, G. Del Giudice, A. Carravetta, Fine tuning of a PAT hydropower plant in a water supply network to improve the system effectiveness, J. Water Resour. Plan. Manag. (2018) (in press).
[49] Y. Tung, D. Ph, Reliability Assessment and Risk Analysis, n.d.
[50] J.L. Romeu, Practical reliability engineering, Technometrics 45 (2003), https://doi.org/10.1198/tech.2003.s133, 173–173.
[51] T. Williams, Probability and statistics with reliability, queueing and computer science applications, J. Oper. Res. Soc. 34 (1983) 916–917, https://doi.org/10.1198/tech.2003.s25.
[52] H. Barringer, A life cycle cost summary, in: Conf. Maint. Soc, 2003, pp. 1–10. http://scholar.google.com/scholar?hl=en&btnG=Search&q=intitle:A+Life+Cycle+Cost+Summary#0%5Cnhttp://scholar.google.com/scholar?hl=en&btnG=Search&q=intitle:A+life+cycle+cost+summary%230.
[53] H.P. Barringer, Life cycle cost and good practices, Npra Maint. Conf. (1998) 1–26.
[54] O. Fecarotta, A. Carravetta, H.M. Ramos, R. Martino, An improved affinity model to enhance variable operating strategy for pumps used as turbines, J. Hydraul. Res. 1686 (2016) 1–10, https://doi.org/10.1080/00221686.2016.1141804.
[55] A. Carravetta, M.C. Conte, O. Fecarotta, H.M. Ramos, Evaluation of PAT performances by modified affinity law, Procedia Eng. 89 (2014) 581–587, https://doi.org/10.1016/j.proeng.2014.11.481.
[56] C.S. Lai, M.D. McCulloch, Levelized cost of electricity for solar photovoltaic and electrical energy storage, Appl. Energy 190 (2017) 191–203, https://doi.org/10.1016/j.apenergy.2016.12.153.
[57] V. Tutterow, L. Berkeley, Going with the Flow : life cycle costing for industrial pumping systems, in: ACEEE Summer Study Energy Effic. Ind, vol. 2, ACEEE, Tarrytown, NY, 2001.
[58] Xylem FLYGT, Life Cycle Costs (LCC) for Wastewater Pumping Systems, 2015. https://www.xylem.com/siteassets/support/white-papers/white-papers-pdf/life-cycle-costs-lcc-for-wastewater-pumping-systems.pdf.
[59] U.S. Department of Energy - DOE Office of Indian Energy, Levelized Cost of Energy (LCOE), 2015. https://energy.gov/sites/prod/files/2015/08/f25/LCOE.pdf.
[60] K. Branker, M.J.M. Pathak, J.M. Pearce, A review of solar photovoltaic levelized cost of electricity, Renew. Sustain. Energy Rev. 15 (2011) 4470–4482, https://doi.org/10.1016/j.rser.2011.07.104.